New organic metals based on BDH–TTP radical cation salts with the photochromic nitroprusside anion [FeNO(CN)(5)](2-)

10 AUTHORS, INCLUDING:

Salavat Khasanov
Institute of Solid State Physics RAS
303 PUBLICATIONS **2,556** CITATIONS

SEE PROFILE

Sergey Simonov
Institute of Solid State Physics RAS
74 PUBLICATIONS **463** CITATIONS

SEE PROFILE

Rimma Shibaeva
Institute of Solid State Physics RAS
228 PUBLICATIONS **1,724** CITATIONS

SEE PROFILE

New Organic Metals Based on BDH-TTP Radical Cation Salts with the Photochromic Nitroprusside Anion [FeNO(CN)$_5$]$^{2-}$**

By *Irina Shevyakova, Lev Buravov, Vladislava Tkacheva, Leokadiya Zorina, Salavat Khasanov, Sergey Simonov, Juni-chi Yamada, Enric Canadell,* Rimma Shibaeva,** and *Eduard Yagubskii**

Three new 2,5-bis(1,3-dithiolan-2-ylidene)-1,3,4,6-tetrathiapentalene (BDH-TTP) radical cation salts with the photochromic nitroprusside anion have been synthesized: κ-(BDH-TTP)$_4$[FeNO(CN)$_5$]·NB (**1**), κ-(BDH-TTP)$_4$[FeNO(CN)$_5$] (**2**), and (BDH-TTP)$_2$[FeNO(CN)$_5$] (**3**). The salts were characterized by single-crystal X-ray diffraction, electrical resistance measurements, and electronic band structure calculations. The crystals of **1** and **2** have a layered structure in which the BDH-TTP layers of κ-type alternate with anionic sheets. Solvent (nitrobenzene) molecules are also involved in the composition of the anion sheet of **1**. The crystals of **1** have triclinic symmetry and two crystallographically independent BDH-TTP radical cations in the unit cell, while there is only one independent radical cation in the monoclinic structure of **2**. The salts **1** and **2** are stable quasi-2D metals down to 4.2 K, while **3**, with full charge transfer, is a semiconductor with low conductivity at room temperature. It is suggested that the κ-type layers of BDH-TTP are more robust than those of BEDT-TTF and its derivatives and the consequences for the electronic structure are discussed.

1. Introduction

Until the end of the twentieth century all known low-dimensional molecular superconductors were based on radical ion salts of organic π-donors or metal-complex π-acceptors (M(dmit)$_2$ salts), which were tetrachalcogenafulvalene derivatives.[1] Most of the quasi-2D superconductors are radical cation salts of bis(ethylenedithio)tetrathiafulvalene (BEDT-TTF). A very important and challenging question in this field was the

possibility of synthesizing organic superconductors based on π-donors, which did not contain the tetrachalcogenafulvalene fragment. The problem remained unsolved for a long time. An important step forward was made in 1999, with the synthesis of a structural isomer of BEDT-TTF, 2,5-bis(1,3-dithiolan-2-ylidene)-1,3,4,6-tetrathiapentalene (BDH-TTP), which is a derivative of 2,5-bis(methylene)-1,3,4,6-tetrathiapentalene and does not involve the tetrathiafulvalene fragment.[2]

BEDT-TTF   BDH-TTP
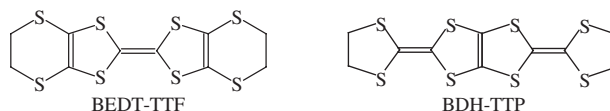
It was found that BDH-TTP forms 2:1 radical cation salts with monoanions of different geometries (linear, tetrahedral, and octahedral), which are metals down to 2.0 K independent of the anion geometry. The crystal structures of the "metallic" salts (BDH-TTP)$_2$X (X = PF$_6$, FeCl$_4$) are characterized by the presence of κ-type BDH-TTP layers alternating with anion sheets.[2,3] The main structural differences between the BDH-TTP and BEDT-TTF molecules are the following: i) BDH-TTP is a more planar molecule than BEDT-TTF and ii) the terminal ethylene groups of BDH-TTP are part of rigid five-membered rings, while those of BEDT-TTF are part of more flexible six-membered rings which allow the BEDT-TTF molecule to be in different conformations. To enhance the structural flexibility of BDH-TTP, its dithiane analog, namely, 2,5-bis(1,3-dithian-2-ylidene)-1,3,4,6-tetrathiapentalene (BDA-TTP), was synthesized in 2001 and radical cation salts based on this donor with anions of different geometries were prepared.[4] The investigation of the structural, conducting, and magnetic properties of these salts showed that those with octahedral anions, (BDA-TTP)$_2$X (X = PF$_6$, AsF$_6$, SbF$_6$), have layered structures of β-type and are superconductors with critical temperatures

[*]   Dr. E. Canadell
      Institut de Ciència de Materials de Barcelona (CSIC)
      Campus de la U.A.B.
      E-08193 Bellaterra (Spain)
      E-mail: canadell@icmab.es
      Dr. R. P. Shibaeva, Dr. S. S. Khasanov, Dr. L. V. Zorina,
      S. V. Simonov
      Institute of Solid State Physics, Russian Academy of Sciences
      142432 Chernogolovka, MD (Russia)
      E-mail: shibaeva@issp.ac.ru
      Dr. E. B. Yagubskii, I. Yu. Shevyakova, Dr. L. I. Buravov,
      Dr. V. A. Tkacheva
      Institute of Problems of Chemical Physics
      Russian Academy of Sciences
      142432 Chernogolovka, MD (Russia)
      E-mail: yagubski@icp.ac.ru
      Dr. J. Yamada
      Department of Material Science, Graduate School of Science
      Himeji Institute of Technology
      3-2-1 Kouto, Kamigori-cho, Ako-gun, Hyogo 678–1297 (Japan)

$T_c = 5.9$–7.5 K at ambient pressure while the salt with the $GaCl_4^-$ tetrahedral anion, β-(BDA-TTP)$_2$GaCl$_4$, is superconductor ($T_c = 3.1$ K) at pressure $P = 8.3$ kbar.[5] Thus, a new family of low-dimensional organic superconductors based on π-donors, which did not contain the tetrachalcogenafulvalene fragment was found. However, the effect of the nature of the anion on the structure and properties of the BDH-TTP- and BDA-TTP-based salts has been only partially studied so far, and the synthesis of new salts based on these donors, as well as the study of their structures and properties, is of great interest.

We considered the possibility of preparing radical cation salts of BDH-TTP and BDA-TTP with the photochromic nitroprusside (NP) anion, [FeNO(CN)$_5$]$^{2-}$. The use of NP as a counterion in these salts is associated with the design of multifunctional materials, which would combine (super)conductivity and photochromism.[6–15] Here we report the preparation, crystal and electronic structures, as well as the conducting properties, of three new BDH-TTP salts with the NP-anion, κ-(BDH-TTP)$_4$[FeNO(CN)$_5$]·NB (1), κ-(BDH-TTP)$_4$[FeNO(CN)$_5$] (2), and (BDH-TTP)$_2$[FeNO(CN)$_5$] (3). In contrast with these results, attempts to synthesize BDA-TTP salts with the NP counterion were unsuccessful.

2. Results and Discussion

The salts **1**–**3** were synthesized using the electrocrystallization method. Nitrobenzene, benzonitrile, and 1,1,2-trichloroethane were used as solvents. It was found that the nature of the solvent and electrolyte, current value, and temperature strongly affect the crystal composition and quality. Crystals of **1**, **2**, and **3** that were suitable in quality for X-ray analysis were prepared at elevated temperature (55 °C) in nitrobenzene using K$_2$[FeNO(CN)$_5$]·2H$_2$O as a supporting electrolyte. The crystals grew on the anode as very thin black plates. The elevated electrocrystallization temperature was used because of the low solubility of BDH-TTP. The crystals of **1** comprising the solvent molecule (nitrobenzene) were formed at current $I = 0.2$ μA, while the crystals of **2** and **3** grew on the electrode in both nitrobenzene and other solvents (trichloroethane, benzonitrile) at higher currents ($I \simeq 0.4$ μA). Usually, the crystals of only one phase, either **1**, **2**, or **3** were formed in the syntheses.

The crystals of **1** and **2** have a layered structure in which the BDH-TTP layers alternate with anionic sheets (Figs. 1,2). Solvent (nitrobenzene) molecules are also involved in the composition of the anion sheet of **1**. The crystals of **1** have triclinic symmetry and two crystallographically independent BDH-TTP radical cations (I and II) in the unit cell, while there is only one independent radical cation in the monoclinic structure of **2**. The atom labeling for the anions and radical cations is shown in Figure 3. The distribution of bond lengths in the BDH-TTP radical cations (Table 1) is similar in both structures and corresponds to BDH-TTP$^{0.5+}$. The tendency to exhibit longer double C=C bonds and shorter single S–C bonds with increasing charge on the cation, which is characteristic of BEDT-TTF and its derivatives, is also observed in BDH-TTP. For example, in BDH-TTP^0 the C=C bond is 1.319(5) Å in the TTP fragment,
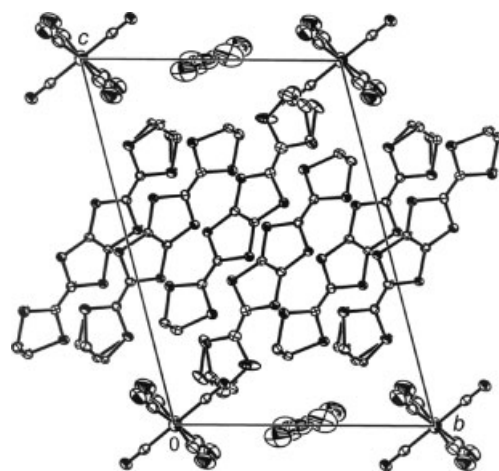
Figure 1. Projection of the crystal structure of κ-(BDH-TTP)$_4$[NP]·NB (**1**) along the *a*-direction.
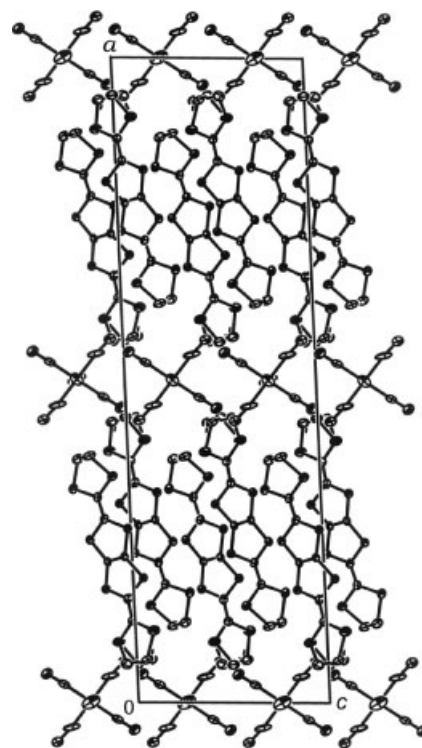
Figure 2. Projection of the crystal structure of κ-(BDH-TTP)$_4$[NP] (**2**) along the *b*-direction.

and 1.344(5) Å between the TTP fragment and 1,3-dithiolane cycles,[2] while these bonds in the monocharged cation are 1.375(7) and 1.364(5) Å, respectively in the (BDH-TTP)[Fe(i-soquinoline)$_2$(NCS)$_4$] salt.[16] It is remarkable that the double C=C bond in the TTP fragment is the most sensitive to the charge. The values for this bond: 1.356(5) Å for BDH-TTP I and 1.350(5) Å for BDH-TTP II in the structure of **1**, and 1.347(5) Å in the structure of **2**, as well as the values of other double C=C bonds (Table 1) are intermediate between those

standable when taking into account the nature of the highest occupied molecular orbital (HOMO) of BDH-TTP.

HOMO BDH-TTP

According to our calculations, the HOMO is bonding in the region of the three C=C bonds. However, whereas the coefficients of the Cp$_z$ orbitals are identical and large for the C=C bond in the TTP fragment, the two coefficients are quite different, one being clearly smaller, for the double bonds between the TTP fragment and 1,3-dithiolane cycles. Consequently the overlap population (and thus, the bond strength) of the C=C in the TTP fragment decreases more rapidly when depopulating the HOMO. This is a consequence of the fact that the outer double bonds are perpendicular to the central one, allowing the mixing of the π-HOMO of the central C$_2$S$_4$ core with both the π- and π*-orbitals of the outer C=C double bonds. Since the mixing with π* must be in phase whereas the mixing with π must be out of phase, the coefficient of the carbon nearest to the the central C$_2$S$_4$ core becomes smaller whereas the other becomes larger.

The radical cations in both salts have the same conformation: they exhibit a noticeable bending of the molecule, and disorder, which is retained even at low temperatures, is observed for the ethylene groups on one side of BDH-TTP, while the other part of the molecule remains ordered and almost planar. The dihedral angles of bending along the S–S lines between the three tetrathiaethylene fragments of the donor molecule in **1** are 2.03(6) and 4.35(6)° (BDH-TTP I), and 1.28(6) and 12.69(5)° (BDH-TTP II) for the ordered and disordered sides of the molecule, respectively (Fig. 4). For **2** the corresponding angles are 2.51(6)° and 8.52(6)°. Thus, the BDH-TTP radical cations are very similar in both salts.

Figure 4. Conformation of the BDH-TTP radical cations in the structures **1** and **2**.

The radical cation layers in the crystals of **1** and **2** have the same κ-type packing motif, i.e., they are built of centrosymmetrical dimers positioned relative to each other at angles of 80.44(3)° and 83.32(3)°, respectively. In contrast to **2**, the radical cation layers in the structure of **1** comprise two independent BDH-TTP dimers, I–I$_i$ and II–II$_i$ (Fig. 5a). For both salts there is an almost direct overlapping of radical cations of the "bond-over-ring"-type characteristic of BDH-TTP, with a very small shift along the longer molecular axis (Fig. 5b). The interplanar distances are almost the same in the dimers, 3.39(3) and 3.44(4) Å in **1**, and 3.46(3) Å in **2**. The relatively small distances between the mean planes of the BDH-TTP molecules
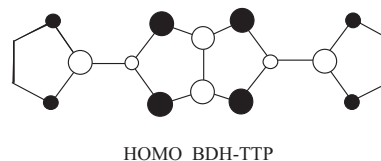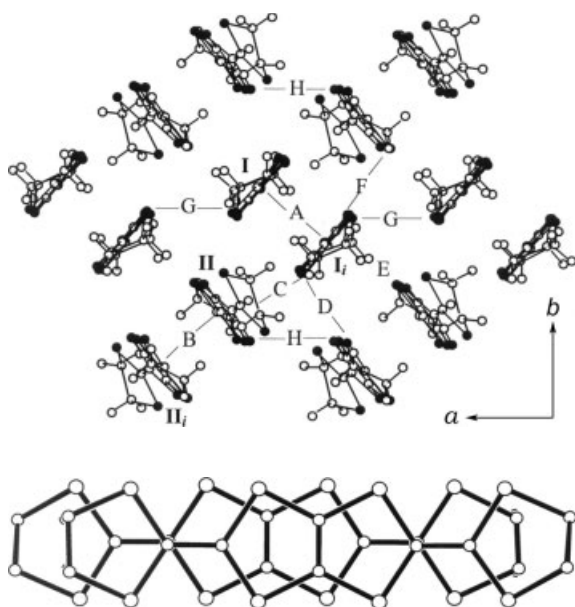
Figure 3. Atom labeling for the [NP]-anions in the structures **1** (a) and **2** (b) and for BDH-TTP in **2** (c). In **1** the corresponding atoms for the BDH-TTP radical cations I and II have the numbers S11–S18, C11–C20 and S21–S28, C21–C30, respectively.

Table 1. Bond lengths (*d*, Å) for the BDH-TTP radical cations in **1** and **2**.

κ-(BDH-TTP)$_4$[NP]·NB (**1**)				κ-(BDH-TTP)$_4$[NP] (**2**)	
BDH-TTP I		BDH-TTP II			
Bond	*d*	Bond	*d*	Bond	*d*
S11 C11A	1.817(5)	S21 C21A	1.831(4)	S1 C1A	1.792(4)
S11 C11B	1.78(3)	S21 C21B	1.798(5)	S1 C1B	1.793(5)
S11 C13	1.745(4)	S21 C23	1.744(4)	S1 C3	1.744(4)
S12 C12A	1.824(6)	S22 C22A	1.803(4)	S2 C2A	1.792(5)
S12 C12B	1.78(3)	S22 C22B	1.825(5)	S2 C2B	1.793(5)
S12 C13	1.744(4)	S22 C23	1.750(4)	S2 C3	1.742(4)
S13 C14	1.764(4)	S23 C24	1.761(4)	S3 C4	1.765(4)
S13 C15	1.734(4)	S23 C25	1.744(4)	S3 C5	1.736(3)
S14 C14	1.757(4)	S24 C24	1.766(4)	S4 C4	1.765(4)
S14 C16	1.738(3)	S24 C26	1.735(4)	S4 C6	1.740(4)
S15 C15	1.738(4)	S25 C25	1.736(4)	S5 C5	1.740(4)
S15 C17	1.769(4)	S25 C27	1.759(4)	S5 C7	1.756(3)
S16 C16	1.738(4)	S26 C26	1.745(3)	S6 C6	1.738(3)
S16 C17	1.768(4)	S26 C27	1.777(4)	S6 C7	1.766(4)
S17 C18	1.756(4)	S27 C28	1.760(4)	S7 C8	1.736(4)
S17 C19	1.815(4)	S27 C29	1.820(4)	S7 C9	1.807(4)
S18 C18	1.750(4)	S28 C28	1.743(4)	S8 C8	1.746(4)
S18 C20	1.825(4)	S28 C30	1.815(4)	S8 C10	1.813(4)
C11A C12A	1.516(9)	C21A C22A	1.504(7)	C1A C2A	1.512(5)
C11B C12B	1.49(5)	C21B C22B	1.50(1)	C1B C2B	1.511(5)
C13 C14	1.368(5)	C23 C24	1.365(5)	C3 C4	1.353(5)
C15 C16	1.356(5)	C25 C26	1.350(5)	C5 C6	1.347(5)
C17 C18	1.348(5)	C27 C28	1.354(5)	C7 C8	1.367(5)
C19 C20	1.508(5)	C29 C30	1.523(5)	C9 C10	1.509(6)

for BDH-TTP$^{0[2]}$ and BDH-TTP$^{1+[16]}$ and close to the values for BDH-TTP in (BDH-TTP)$_2$PF$_6$$^{[2]}$ The larger sensitivity to the charge of the C=C bond in the TTP fragment is under-

Figure 5. a) Projection of the radical cation layer of **1** along the long axis of the BDH-TTP molecule. b) Overlap mode in the BDH-TTP dimers.

result in shortened intermolecular S···S, S···C, and C···C contacts inside the dimers. The short intermolecular S···S distances in the layer are listed in Table 2. The contacts are distributed uniformly within the layer and form an extended two-dimensional network leading to strong interactions and high conductivity for the radical cation layer.

Table 2. Short S···S ($r \leq 3.70$ Å) contacts [Å] and absolute values of the intermolecular interaction $\beta_{HOMO-HOMO}$ energies [eV] in the radical cation layers of **1** and **2**.

	1		**2**	
	S···S	$\beta_{HOMO-HOMO}$	S···S	$\beta_{HOMO-HOMO}$
A	3.595 (×2), 3.617 (×2)	0.4069	3.619 (×2)	0.3613
B	3.662 (×2)	0.3061	B = A	
C	3.509, 3.670	0.1318	3.509, 3.587	0.1476
D	3.554, 3.573, 3.577, 3.595, 3.661	0.0491	3.548, 3.549, 3.625, 3.634, 3.663	0.0742
E	3.488, 3.683	0.1366	E = C	
F	3.439, 3.499, 3.540, 3.587, 3.595	0.0386	F = D	
G	–	0.2125	3.542 (×2)	0.2420
H	3.653 (×2)	0.1995	H = G	

Disorder is observed in the anion sheets of both **1** and **2**. For instance in **1** non-centrosymmetrical NP anions and nitrobenzene molecules are located in centers of symmetry. Because of this, the atoms of the NO group of the anion and the NO_2 group of the solvent are equiprobably distributed in two positions. Since the positions of the *trans*-CN and NO ligands are not separated, the analysis of the bond lengths in the Fe–N–O fragment, responsible for the photochromic properties, is impossible. There is a translational disorder in the anion sheet of

2, and the positions of the NP anions are half-populated. It is most likely that the *b*-parameter must be doubled, something that is justified by the observation of additional superstructural lines in Weissenberg and rotation X-ray photographs. However, the diffusion character of the superstructural reflections does not allow them to be used in the X-ray analysis. Moreover, there is a disorder in the anions, which is associated with the position of the NO group. All the Fe–C distances are ~1.85 Å, shorter than the equivalent distances found for the NP anion in other salts (Fe–C = 1.91 Å), i.e., all of the six CN positions of the coordination sphere of Fe contain NO atoms as an admixture.

A detailed comparative analysis of the structures of **1** and **2** showed that in spite of the different structure and composition of their anion sheets, the internal structure of the radical cation layer is almost the same in both salts. In this respect, the BDH-TTP salts are essentially different from the BEDT-TTF ones in which the nature of the anion strongly affects the structure of the radical-cation layer. For example, in the BEDT-TTF salts with the photochromic $[RuNOX_5]^{2-}$ (X = Br, Cl) anion, the intercalation of solvent molecules in the anion sheet results in drastic changes in the structure of the radical cation layer of BEDT-TTF.[17]

In contrast to the layered salts **1** and **2**, the completely ionic salt (BDH-TTP)$_2$[FeNO(CN)$_5$] contains almost isolated stacks of radical cations BDH-TTP$^+$ (Fig. 6a). The stacks are strongly dimerized, the interplanar distance being 3.38(1) Å in the dimer and 3.74(1) Å between the dimers. There are four S···S [3.392(3) and 3.597(3) Å] and two C···C [3.49(1) Å] intradimer short intermolecular contacts in the stack (Fig. 6b) and only one interstack S···S contact of 3.380(3) Å. The $\beta_{HOMO-HOMO}$ interaction energies[18] for the intra- and interdimer interactions along the stacks are calculated to be 0.7347 and 0.1850 eV, re-
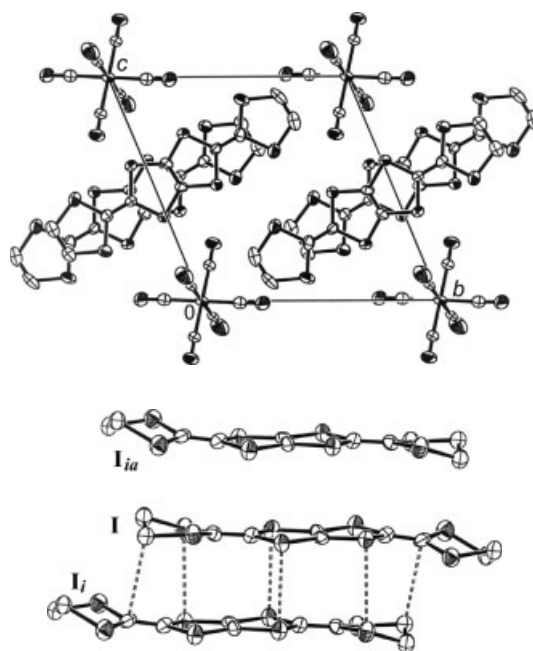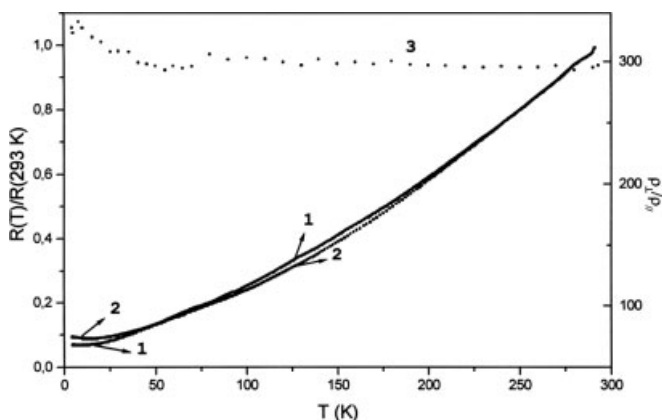

Figure 6. a) Projection of the crystal structure of (BDH-TTP)$_2$[NP] (**3**) along the *a*-direction. b) Side view of the radical cation stack.

spectively, in agreement with the structural analysis. The values for the interstack interactions are between one and two orders of magnitude smaller. The calculated band structure contains two HOMO bands exhibiting dispersion along the stacks direction and well separated by a large dimerization gap. The bands are quite flat along the interstack directions so that salt **3** should be considered as a quasi-one-dimensional semiconductor made of moderately interacting (BDH-TTP$^+$)$_2$ dimers.

The nitroprusside anions in salt **3** are located at the inversion centers and are disordered: the NO atoms are included in four of the six CN positions, something that agrees with the shortened lengths of the corresponding Fe–C bonds (~ 1.87 Å). Many intermolecular contacts of the S$\cdots$N (2.880–3.416 Å) and C–H$\cdots$N (2.39–2.64 Å) types are found between the radical cations and the anions.

The crystals of (BDH-TTP)$_2$[FeNO(CN)$_5$] **3** have low conductivity at room temperature ($\sigma \sim 10^{-4}$ Ω^{-1} cm^{-1}) and show a semiconducting behavior upon cooling. This is in agreement with the completely ionic state of BDH-TTP and charge localization within the dimers. In contrast, salts **1** and **2** with donors in a partially oxidized state are stable quasi-two-dimensional metals whose room-temperature conductivity in the plane of the BDH-TTP layers is 3.0–6.0 Ω^{-1} cm^{-1}. The conductivity of **1** and **2** in the direction perpendicular to the conducting donor layers is approximately three orders of magnitude lower, something which indicates a strong two-dimensional character of the conductivity. The temperature dependence of the resistivity for both salts is similar (Fig. 7) and show a metallic behavior down to liquid-helium temperature (4.2 K). The anisotropy of the resistivity ($\rho_\perp/\rho_\parallel$) remains almost unchanged down to 4.2 K (Fig. 7). The absence of superconductivity is probably a result of the orientational disorder in the conducting layers of BDH-TTP, which is retained at low temperatures. Superconductivity in low-dimensional organic conductors is known to be very sensitive to disorder.[19]

The band structures and Fermi surfaces for **1**, **2**, κ-(BDH-TTP)$_2$PF$_6$,[2] and κ-(BDH-TTP)$_2$FeCl$_4$[3] have been calculated. Those for **1** and **2** are reported in Figures 8,9, respectively. Except for some minor differences in the band structures, the results for the κ-(BDH-TTP)$_2$PF$_6$ and κ-(BDH-TTP)$_2$FeCl$_4$ salts
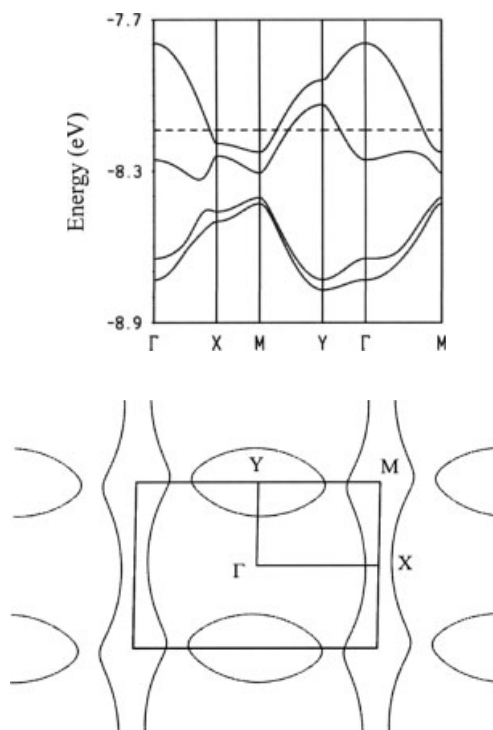
Figure 8. a) Band structure and b) Fermi surface calculated for the donor layers of κ-(BDH-TTP)$_4$[NP]·NB (**1**). The dashed line in (a) refers to the Fermi level and $\Gamma = (0, 0)$, $X = (a^*/2, 0)$, $Y = (0, b^*/2)$, $M = (a^*/2, b^*/2)$, and $S = (-a^*/2, b^*/2)$.
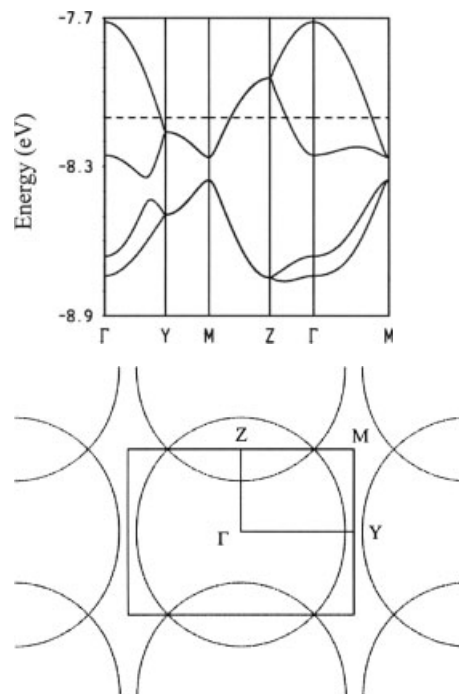
Figure 7. 1,2) Temperature dependencies of relative resistivity for single crystals of κ-(BDH-TTP)$_4$[NP]·NB (**1**) and κ-(BDH-TTP)$_4$[NP] (**2**), respectively, measured along the BDH-TTP conducting layers. 3) Temperature dependence of anisotropy of resistivity ($\rho_\perp/\rho_\parallel$) for κ-(BDH-TTP)$_4$[NP]·NB.

Figure 9. a) Band structure and b) Fermi surface calculated for the donor layers of κ-(BDH-TTP)$_4$[NP] (**2**). The dashed line in (a) refers to the Fermi level and $\Gamma = (0, 0)$, $Y = (b^*/2, 0)$, $Z = (0, c^*/2)$, and $M = (a^*/2, b^*/2)$.

are practically identical with those of Figure 9 and, thus, are not reported here. The repeat unit of the donor layers in **1** and **2**, as for all κ-phases, contains four donors so that the band structures of Figures 8 and 9 contain four bands mainly built from the HOMO of BDH-TTP. The main difference in the donor layers of the two salts is that whereas those of salt **1** contain two different dimers I–I$_i$ and II–II$_i$, those of salt **2** (like those of the κ-(BDH-TTP)$_2$PF$_6$ and κ-(BDH-TTP)$_2$FeCl$_4$ salts) contain only one type of dimer I–I$_i$ (and one type of donor). As a result, both the topology of the Fermi surface and the number of the HOMO⋯HOMO interactions is different. In both cases, the Fermi level cuts two bands so that the Fermi surfaces contain formally a closed hole portion (around Y and Z in **1** and **2**, respectively) and an open electron portion (along the X→M and Y→M directions in **1** and **2**, respectively). Both the nature of the Fermi surface and the bandwidths are very similar to those of metallic κ-phases of BEDT-TTF and its derivatives,[20] so that it is understandable that both salts are found to exhibit a metallic behavior. Despite the obvious similarities between the band structures and Fermi surfaces of the two salts, there are differences which are interesting to look at.

In a donor layer of the κ-type there are three different types of intermolecular donor⋯donor interactions: i) the intradimer interactions (A and B in Fig. 5a), ii) those implicating donor molecules which are almost parallel to each other and belonging to different dimers (G and H in Fig. 5a), and iii) those associated with donors which are almost orthogonally oriented (C, D, E, and F in Fig. 5a). The layers in **1** contain two different dimers and two different donors. In contrast, the donor layer of **2** contains only one type of dimer and one type of donor. In the donor layer of **2**, because of the equivalence of the two dimers, interactions A and B, as well as C and E, D and F, and G and H, are equivalent. Thus, instead of eight different HOMO⋯HOMO interactions present in the donor layer of **1**, there are only four in that of **2**. There is still a third different type of layer with the κ-type topology which is intermediate between those of these two salts: layers like those in κ-(BEDT-TTF)$_2$-Cu(NCS)$_2$[21] as well as in κ-(BEDT-TTF)$_2$Cu(CN)[N(CN)$_2$][22] are built from only one type of dimer, I–II, made of two different donors. In that case, the number of different HOMO⋯HOMO interactions is six, intermediate between the number for **1** and **2**. The decrease in the different number of HOMO⋯HOMO interactions is, of course, related to an increase on the symmetry of the layer which in turn influences the nature of the band structure. Because of the presence of dimers, the four HOMO bands of κ-phases appear as two pairs of bands the upper one being partially filled. Since the average charge of the donors is +1/2, there must be two holes in the upper pair of bands. For κ-type layers in which there is only one type of dimer and one type of donor, the two bands of a pair must be degenerate all along both directions at the border of the Brillouin zone which are parallel to the main axes of reciprocal space (i.e., the X→M and M→Y directions in Fig. 9a). In the case of κ-type layers in which there is only one type of dimer but two types of donors, the two bands of a pair must be degenerate all along only one of the two directions at the border of the Brillouin zone which are parallel to the main axes of recip-

rocal space (see for instance the Fermi surface for the donor layers of κ-(BEDT-TTF)$_2$Cu(NCS)$_2$[21]). A practical consequence of this symmetry lowering and degeneracy leaving is that whereas in the first case the closed and open portions of the Fermi surface touch at one of the borders of the Brillouin zone (see Fig. 9b, for instance), they do not in the second case (see for instance the Fermi surface for the donor layers of κ-(BEDT-TTF)$_2$Cu(NCS)$_2$[21]). The consequences of such gap opening (usually relatively small) because of the lowering in symmetry are clearly seen in the magnetoresistance experiments. In the case of κ-type layers in which there are two types of dimers and two types of donors, the degeneracy along the two directions at the border of the Brillouin zone which are parallel to the main axes of reciprocal space are lost. In other words, the two upper bands are really two different bands (as it is the case of the two upper bands in Fig. 8a). The separation between the two bands will increase with the difference between the two dimers (and their interaction with other dimers). In principle the two bands can be very similar, retaining the main characteristics of the band structure and Fermi surface of the usual κ-phases, or can be strongly separated leading to a very small or even no overlap at all. In the latter case the metallic state could be lost either because of the creation of a bandgap or because the overlap is weak leading to a small number of carriers which localize in the presence of disorder. An example of this third class of κ-phases among BEDT-TTF salts is κ-(BEDT-TTF)$_4$[RuNOX$_5$]·C$_6$H$_5$CN (X = Cl, Br)[17] in which the two dimers are very different and show activated conductivity. In that case both from the structural and electronic viewpoints the two dimers are very different. For instance, the mode of overlap in the two dimers and as a result the HOMO⋯HOMO interaction, as measured by the $\beta_{HOMO-HOMO}$ interaction energies are also very different (0.617 and 0.233 eV).[17] The other known examples are the radical cation salts of the κ-(BEDT-TTF)$_4$M(CN)$_6$·3H$_2$O family (M = Fe^{III}, Co^{III}, Cr^{III})[23] and the low-temperature phase of κ-(BEDT-TTF)$_4$PtCl$_6$·C$_6$H$_5$CN[24] in which there are also two different dimers and donors and the conductivity is again activated. In the latter case the difference between the two intradimer $\beta_{HOMO-HOMO}$ is not as large, but in addition several of the interdimer interactions are clearly smaller than in usual κ-phases.[24c] Band-structure calculations for both the κ-(BEDT-TTF)$_4$[RuNOX$_5$]·C$_6$H$_5$CN (X = Cl, Br)[17] and κ-(BEDT-TTF)$_4$PtCl$_6$·C$_6$H$_5$CN[24c] salts showed that the overlap between the upper pair of bands was completely or almost completely lost, in agreement with our discussion. To the best of our knowledge these are the only previously known κ-phases belonging to the third category.

The absolute values of the $\beta_{HOMO-HOMO}$ interaction energies for salts **1** and **2** are reported in Table 2. The difference in the intradimer interactions is not so large and definitely very far from that in κ-(BEDT-TTF)$_4$[RuNOBr$_5$]·C$_6$H$_5$CN. The other interactions are comparable in both salts. For other κ-salts of BDH-TTP like κ-(BDH-TTP)$_2$PF$_6$ and κ-(BDT-TTP)$_2$FeCl$_4$, the corresponding values are: 0.3330 and 0.3472 for the A (= B; intradimer) interaction, 0.2156 and 0.2530 for the G (= H) interaction, 0.1207 and 0.1091 for the C (= E) interaction and 0.0868

and 0.1012 for the D (= F) interaction. It is clear that the donor layers of the κ-salts of BDH-TTP are electronically very similar, a remarkable difference with respect to those of BEDT-TTF and its derivatives. As a result, even if salt **1** belongs to the third category of κ-salts, the differences between the two dimers are weak enough so as to retain the main electronic characteristics of the κ-phases and consequently, the metallic behavior. As it is clear from the similarity in $\beta_{HOMO-HOMO}$ interaction energies, which are very sensitive to the details of the donor layer structure, the κ-type layer of the BDH-TTP salts seems to be quite robust. Even inclusion of a solvent molecule in between the anions does not strongly disturb it. The robustness of the donor lattices of salts of these fused tetrathiafulvalene-type donors was also recently noticed in the case of the β-type layers of BDT-TTP.[25] The greater sensitivity of the BEDT-TTF and its derivatives to the nature of the counterion layers stems from the fact that the terminal ethylene groups are part of very flexible six-membered rings which confer them a great conformational adaptability; in contrast, by being part of five-membered rings in BDH-TTP, these terminal ethylene groups are much more rigid and the donor is more planar, leading to a more compact and rigid packing of the donors.

Finally, let us note that the Fermi surface of salt **1** while sharing most of the features of the Fermi surface of typical κ-phases exhibits some interesting aspects. Since the separation between the closed and open portions is larger than in usual κ-phases with one type of dimer but two different donors,[20] it is very similar to that of typical α-phases. Remarkably, the closed part of the Fermi surface shares two features with that of the Fermi surface of several α-phases:(i) the area is very similar (16.8 % in the present case) and ii) it is somewhat tilted along the long axis. Thus the Fermi surface of salt **1** shares aspects of both those of typical κ- and α-phases though the structure of the layer is that of a κ-phase. It is clear that the answer provided by the inclusion of the solvent molecule has been softened because of the rigidity of the donor lattice inducing an original situation among κ-phases. Since the metallic state is retained down to low temperatures, the detailed characterization of the Fermi surface of salt **1** through magnetoresistance measurements would be very interesting.

3. Conclusion

Three new salts of the non-tetrathiafulvalene containing BDH-TTP donor with the photochromic nitroprusside anion have been prepared. Two of them, κ-(BDH-TTP)₄[Fe-NO(CN)₅] and κ-(BDH-TTP)₄[FeNO(CN)₅]·NB exhibit metallic behavior down to low temperatures. Remarkably, introduction of the solvent molecule within the anionic sheets perturbs the donor layers in a minor way, something which contrasts with the situation for BEDT-TTF and its derivatives. The terminal ethylene groups are much more rigid in BDH-TTP because they are part of five-membered rings and the donor is more planar, leading to a more compact and rigid packing of the donors. κ-(BDH-TTP)₄[FeNO(CN)₅]·NB is the first κ-phase with two different dimers and donors which exhibits

metallic behavior. Attempts to prepare κ-type salts of BDH-TTP with the $RuNOX_5^{2-}$ (X = Cl, Br) and $PtCl_6^{2-}$ anions (including solvent molecules) would be very interesting.

4. Experimental

Synthesis: The donor BDH-TTP and the electrolyte K₂[FeNO(CN)₅] were prepared according to previously reported methods [2,26]. BDH-TTP radical-cation salts were synthesized on a platinum wire electrode by the electrochemical oxidation of the donor in a H-shaped cell under constant low current at 55 °C. The crystallization time was 5–6 days. The conditions for the synthesis of the salts **1**–**3** are summarized in Table 3.

Table 3. Conditions for the synthesis of the radical cation salts **1**–**3**.

Salt	Reagents [mol L⁻¹]	Solvent [mL]	I [μA]
1 κ-(BDH-TTP)₄[NP]·NB	BDH-TTP: 1.3 × 10⁻³ K₂[NP]·2H₂O: 2.4 × 10⁻³ 18-crown-6: 4.9 × 10⁻³	NB: 20 [a] EtOH: 2 [b]	0.2
2 κ-(BDH-TTP)₄[NP] [c]	BDH-TTP: 1.3 × 10⁻³ K₂[NP]·2H₂O: 2.4 × 10⁻³	NB: 20, EtOH: 2 or	0.3–0.4
3 (BDH-TTP)₂[NP]	18-crown-6: 4.9 × 10⁻³	TCE: 20 [d], EtOH: 2	

[a] NB: nitrobenzene. [b] EtOH: ethanol. [c] The conditions for **2** and **3** are the same. These conditions usually afford crystals of **2**, however in two of the ten syntheses, crystals of **3** were produced. [d] TCE: 1,1,2-trichloroethane.

X-Ray Structure Determination: Experimental X-ray single-crystal diffraction data were collected with an automatic diffractometers Bruker SMART 1K CCD [at room temperature and T = 120 K for crystal **1** and T = 153 K for **2**] and Enraf Nonius CAD4 [at T = 293 K for **3**] by the ω-scan method [λ(Mo Kα) = 0.71073 Å, graphite monochromator]. The main crystallographic and experimental parameters are presented in Table 4. Numerical data corrections were applied for Lorentz and polarization factors. A semi-empirical method was used for absorption correction of the measured intensities in the cases of **1** and **2**. The minimal-to-maximal transmission ratio was 0.94 for crystal sample **3** and the absorption correction was omitted. The crystal structures of **1**–**3** were solved by direct methods with the following Fourier syntheses using the SHELXS-97 program [27]. The positions of the disordered carbon atoms in BDH-TTP radical cations were found from the difference Fourier synthesis. Refinement of the structures of **1**–**3** using the SHELXL-97 program [28] was performed in the anisotropic approximation for all non-hydrogen atoms. The coordinates of the H-atoms were calculated geometrically with isotropic temperature parameters $U_{iso}(H) = 1.2U_{eq}(C)$, where $U_{eq}(C)$ are the equivalent isotropic temperature factors of the corresponding carbon atoms.

Band Structure Calculations: The tight-binding band structure calculations were based upon the effective one-electron Hamiltonian of the extended Hückel method [29]. The off-diagonal matrix elements of the Hamiltonian were calculated according to the modified Wolfsberg–Helmholz formula [30]. All valence electrons were explicitly taken into account in the calculations and the basis set consisted of double-ζ Slater-type orbitals for C and S and single-ζ Slater-type orbitals for H. The exponents, contraction coefficients and atomic parameters for C, S, and H were taken from previous work [31].

Electrical Resistivity Measurements: The direct current (dc) resistivity measurements over the range 4.2–300 K were performed on single crystals using a standard four-probe method with current flow parallel and perpendicular to the BDH-TTP layers. Contacts to the crystals were glued with a graphite paste using 10–20 mm diameter platinum wires. The current applied was 10–20 μA.

Table 4. Crystal data and structure determination details for the radical cation salts κ-(BDH-TTP)₄[NP]·NB **1**, κ-(BDH-TTP)₄[NP] **2**, and (BDH-TTP)₂[NP] **3**.

	1	2	3
I_2 [K] [a]	290(2)	120(2)	153(2)	293(2)
Chemical formula	$C_{51}H_{37}FeN_7O_3S_{32}$	$C_{51}H_{37}FeN_7O_3S_{32}$	$C_{45}H_{32}FeN_6OS_{32}$	$C_{25}H_{16}FeN_6OS_{16}$
Crystal system	Triclinic	Triclinic	Monoclinic	Triclinic
a [Å]	8.271(2)	8.210(1)	38.532(10)	7.442(1)
b [Å]	12.017(3)	11.928(2)	8.038(2)	11.870(2)
c [Å]	18.895(4)	18.681(3)	10.836(3)	11.811(1)
α [deg]	103.981(5)	103.526(3)	90	109.19(1)
β [deg]	101.018(5)	100.759(3)	92.723(6)	92.89(1)
γ [deg]	91.219(5)	91.417(3)	90	110.05(1)
Volume [Å³]	1784.2(7)	1742.9(5)	3352(1)	909.8(2)
Space group, Z	$P\bar{1}$, 1	$P\bar{1}$, 1	$C2/c$, 2	$P\bar{1}$, 1
μ [cm⁻¹] [b]	11.97	12.25	12.65	13.68
Θ range [deg]	1.75–26.05	1.76–25.00	3.19–30.07	2.15–25.00
Index ranges	$-9 \le h \le 10$	$-9 \le h \le 9$	$-51 \le h \le 54$	$-8 \le h \le 8$
	$-14 \le k \le 14$	$-14 \le k \le 14$	$-9 \le k \le 11$	$-14 \le k \le 14$
	$-18 \le l \le 23$	$-22 \le l \le 22$	$-15 \le l \le 15$	$-14 \le l \le 14$
Reflections collected	10 457	11 658	12 648	6321
Independent reflections	6804	6063	4838	3167
R_{int}, R_σ	0.021	0.025, 0.047	0.049, 0.082	0.183, 0.209
No. of variables	399	484	244	223
S [c]	0.877	1.046	0.996	0.989
Final R [$I > 2\sigma(I)$]	0.054	0.044	0.055	0.063

[a] Temperature of X-ray experiment. [b] Linear absorption co-efficient. [c] Goodness of fit on F^2.

[1] T. Ishiguro, K. Yamaji, G. Saito, *Organic Superconductors*, 2nd ed. (Ed: P. Fulde), Springer Series in Solid State Science, Vol. 88, Springer, Berlin **1998**.

[2] J. Yamada, M. Watanabe, H. Anzai, H. Nishikawa, I. Ikemoto, K. Kikuchi, *Angew. Chem. Int. Ed.* **1999**, *38*, 810.

[3] K. Kikuchi, H. Nishikawa, I. Ikemoto, T. Toita, H. Akutsu, S. Nakatsuji, J. Yamada, *J. Solid State Chem.* **2002**, *168*, 503.

[4] J. Yamada, M. Watanabe, H. Akutsu, S. Nakatsuji, H. Nishikawa, I. Ikemoto, K. Kikuchi, *J. Am. Chem. Soc.* **2001**, *123*, 4174.

[5] a) J. Yamada, T. Toita, H. Akutsu, S. Nakatsuji, H. Nishikawa, I. Ikemoto, K. Kikuchi, E. S. Choi, D. Graf, J. S. Brooks, *Chem. Commun.* **2003**, 2230. b) J. Yamada, *J. Phys. IV* **2004**, *114*, 439. c) E. S. Choi, D. Graf, J. S. Brooks, J. Yamada, M. Tokumoto, *J. Phys. IV* **2004**, *114*, 297.

[6] H. Yu, D. Zhu, *Phys. C (Amsterdam, Neth.)* **1997**, *282–287*, 1893.

[7] L. Kushch, L. Buravov, V. Tkacheva, E. Yagubskii, L. Zorina, S. Khasanov, R. Shibaeva, *Synth. Met.* **1999**, *102*, 1646.

[8] M. Gener, E. Canadell, S. S. Khasanov, L. V. Zorina, R. P. Shibaeva, L. A. Kushch, L. I. Buravov, E. B. Yagubskii, *Solid State Commun.* **1999**, *111*, 329.

[9] M. Clemente-Leon, E. Coronado, J. R. Galan-Mascaros, C. Gimenez-Saiz, C. J. Gomez-Garcia, J. M. Fabre, *Synth. Met.* **1999**, *103*, 2279.

[10] L. V. Zorina, S. S. Khasanov, R. P. Shibaeva, M. Gener, R. Rousseau, E. Canadell, L. A. Kushch, E. B. Yagubskii, O. O. Drozdova, K. Yakushi, *J. Mater. Chem.* **2000**, *10*, 2017.

[11] I. Yu. Shevyakova, L. I. Buravov, L. A. Kushch, E. B. Yagubskii, S. S. Khasanov, L. V. Zorina, R. P. Shibaeva, N. V. Drichko, I. Oleiniczak, *Russ. J. Coord. Chem.* **2002**, *28*, 487.

[12] L. V. Zorina, M. Gener, S. S. Khasanov, R. P. Shibaeva, E. Canadell, L. A. Kushch, E. B. Yagubskii, *Synth. Met.* **2002**, *128*, 325.

[13] S. V. Kapelnitsky, E. B. Yagubskii, L. A. Kushch, I. Y. Shevyakova, *JETP Lett.* **2002**, *76*, 165.

[14] R. P. Shibaeva, E. B. Yagubskii, E. Canadell, S. S. Khasanov, L. V. Zorina, L. A. Kushch, T. G. Prokhorova, I. Yu. Shevyakova, L. I. Buravov, V. A. Tkacheva, M. Gener, *Synth. Met.* **2003**, *133–134*, 373.

[15] R. Shibaeva, S. Khasanov, L. Zorina, S. Simonov, I. Shevyakova, L. Kushch, L. Buravov, E. Yagubskii, S. Baudron, C. Mézière, P. Batail, E. Canadell, J. Yamada, *J. Phys. IV* **2004**, *114*, 481.

[16] F. Setifi, S. Golhen, L. Ouahab, A. Miyazaki, K. Okabe, T. Enoki, T. Toita, J. Yamada, *Inorg. Chem.* **2002**, *41*, 3787.

[17] I. Yu. Shevyakova, L. V. Zorina, S. S. Khasanov, L. I. Buravov, V. A. Tkacheva, R. P. Shibaeva, E. B. Yagubskii, E. Canadell, *J. Solid State Chem.* **2002**, *168*, 514.

[18] a) M.-H. Whangbo, J. M. Williams, P. C. W. Leung, M. A. Beno, T. J. Emge, H. H. Wang, *Inorg. Chem.* **1985**, *24*, 3500. b) Since overlap is explicitly included in extended Hückel calculations, these interaction energies (β) should not be confused with the conventional transfer integrals (*t*). Although the two quantities are obviously related and have the same physical meaning, the absolute values of β are somewhat larger than those of *t*.

[19] R. P. Shibaeva, S. S. Khasanov, N. D. Kushch, E. B. Yagubskii, K. Boubekeur, P. Batail, E. Canadell, in *Supramolecular Engineering of Synthetic Metallic Materials* (Eds: J. Veciana, C. Rovira, D. B. Amabillino), Kluwer Academic Publishers, Dordrecht, The Netherlands **1999**, p. 409.

[20] D. Jung, M. Evain, J. J. Novoa, M.-H. Whangbo, M. A. Beno, A. M. Kini, A. J. Schultz, J. M. Williams, P. J. Nigrey, *Inorg. Chem.* **1989**, *28*, 4516.

[21] H. Urayama, H. Yamochi, G. Saito, K. Nozawa, T. Sugano. M. Kinoshita, S. Sato, K. Oshima, A. Kawamoto, J. Tanaka, *Chem. Lett.* **1988**, 55.

[22] H. Yamochi, T. Nakamura, T. Komatsu, N. Matsukawa, T. Inoue, G. Saito, T. Mori, M. Kusunoki, K. Sakaguchi, *Solid State Commun.* **1992**, *82*, 101.

[23] a) P. Maguerès, L. Ouahab, N. Conan, C. J. Gómez-García, P. Delhaès, J. Even, M. Bertault, *Solid State Commun.* **1996**, *97*, 27. b) P. Maguerès, L. Ouahab, P. Briard, J. Even, M. Bertault, L. Toupet, J. Ramos, C. J. Gómez-García, P. Delhaès, T. Mallah, *Synth. Met.* **1997**, *86*, 1859.

[24] a) A. A. Galimzyanov, A. A. Ignatev, N. D. Kushch, V. N. Laukhin, M. K. Makova, V. A. Merzhanov, L. P. Rozenberg, R. P. Shibaeva, E. B. Yagubskii, *Synth. Met.* **1989**, *33*, 81. b) V. E. Korotkov, V. N. Mol-

chanov, R. P. Shibaeva, *Sov. Phys. Crystallogr.* **1992**, *37*, 776. c) M.-L. Doublet, E. Canadell, R. P. Shibaeva, *J. Phys. I* **1994**, *4*, 1479.

[25] a) S. Perruchas, P. Batail, E. Canadell, unpublished. b) S. Perruchas, *Thesis*, École Polytechnique, Palaiseau, France **2003**.

[26] A. N. Gard, P. S. Goel, *Inorg. Chem.* 1971, *10*, 1344.

[27] G. M. Sheldrick, SHELXS-97 — A program for automatic solution of crystal structures, University of Göttingen, Germany **1997**, Release 97-2.

[28] G. M. Sheldrick, SHELXL-97 — A program for crystal structure refinement, University of Göttingen, Germany **1997**, Release 97-2.

[29] M.-H. Whangbo, R. Hoffmann, *J. Am. Chem. Soc.* **1978**, *100*, 6093.

[30] J. Ammeter, H.-B. Bürgi, J. Thibeault, R. Hoffmann, *J. Am. Chem. Soc.* **1978**, *100,* 3686.

[31] A. Pénicaud, K. Boubekeur, P. Batail, E. Canadell, P. Auban-Senzier, D. Jérome, *J. Am. Chem. Soc.* **1993**, *115*, 4101.

_____